1

Block Copolymer Templating as a Path to Porous Nanostructured Carbons with Highly Accessible Nitrogens for Enhanced (Electro)chemical Performance[1]

John P. McGann, Mingjiang Zhong, Eun Kyung Kim, Sittichai Natesakhawat, Mietek Jaroniec, Jay F. Whitacre, Krzysztof Matyjaszewski, and Tomasz Kowalewski

1.1 Introduction

Historically, graphitic and semi-graphitic materials have always played a major role in a wide range of electrical and electrochemical systems. The past two decades have brought some of the most interesting synthetic and processing advances in the area of advanced carbon materials, including the discovery and/or isolation of several sp^2 allotropes (fullerenes, carbon nanotubes, graphene, etc.). In addition, a variety of top-down [1–3] and bottom-up [4] synthetic approaches emerged as a way to control the architecture and chemical functionality.

This, in turn, has led to the development of nanostructured carbons for advanced applications such as supercapacitors, fuel cells, batteries, water-splitting systems, sensors, and gas chemisorbents [5, 6].

In the past, the focus of the field of advanced carbons has been gradually shifting from control over the nanostructure to control over the chemical functionality. One of the most important driving forces in the quest for such "chemical nanocarbons" has been the growing understanding of the electronic properties of graphene. The next breakthroughs in this area can be expected to involve more precise control of the edge states of graphenic domains, including the incorporation of heteroatoms and more complex functionalities [5, 7]. Nitrogen is a particularly attractive heteroatom because of its relative ease of incorporation and abundance in various carbon precursors. Viewed simplistically, nitrogen doping (N-doping) introduces basicity into the carbon structure that can be utilized for a variety of electrochemical and electrocatalytic systems; however, the detailed chemistry behind its effect is still poorly understood. This is largely due to the complexities arising from the heterogeneous nature and, still, relatively ill-defined structure of many of the materials studied. As shown in Figure 1.1, the edge functionalities can be introduced in graphene either through the attachment of pendant groups (e.g., amine, Figure 1.1a) or through edge substitution with heteroatoms (Figure 1.1b,c). Basal plane substitution (quaternary nitrogen, Figure 1.1d) should not significantly impart electrochemical properties [5].

Pyridinic nitrogens (Figure 1.1b) incorporated into the graphitic network are often thought to be the most reactive and beneficial nitrogen-containing functionality for

[1] [8], Reproduced with permission of Wiley.

Chemical Synthesis and Applications of Graphene and Carbon Materials, First Edition.
Edited by Markus Antonietti and Klaus Müllen.

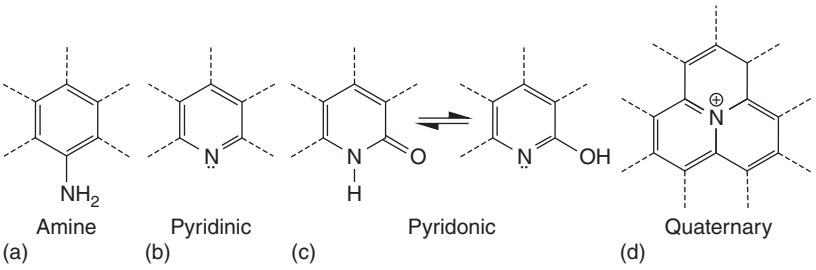

Figure 1.1 Common N-functionalities in graphitic systems. ([8], Reproduced with permission of Wiley.)

electrochemical systems [5]. While there are many synthetic routes to N-doped carbon materials, two key requirements are necessary to fully realize the advantages afforded through graphitic edge N-doping: (i) efficient formation of pyridinic species and (ii) assurance of their (electro)chemical accessibility. The latter could be accomplished by designing material with high-surface area nanoporous structure with pyridinic species preferentially exposed on pore wall surfaces.

In this chapter, we demonstrate how these two requirements can be satisfied simultaneously through the general approach developed in recent years in our laboratories, in which the nanostructure of carbon is templated by the self-assembly of block copolymer or hybrid precursors comprised of a carbon source and a sacrificial block/element [9–23]. In these materials, which will be referred to as copolymer templated nitrogen-rich carbons (CTNCs), high nitrogen content polyacrylonitrile (PAN) is the carbon precursor of choice since its carbonization results in high content of pyridinic functionalities [24]. For block copolymer templating, the sacrificial block needs to be immiscible with the carbon source to assure nanoscale phase separation and formation of well-defined template morphology. Heat treatment results in an N-doped carbon material with morphology replicating the copolymer precursor [9, 11, 13]. As discussed below, copolymer templates of certain compositions afford materials with high surface area and efficient nitrogen exposure to the pore walls, presumably through preferential orientation of PAN chains at the interface with the sacrificial block.

Following a more detailed discussion on the motivation for this choice of templating approach when compared with other methods, this chapter will discuss the structural aspects CTNCs and their performance in applications such as supercapacitors, oxygen-reduction reactions (ORRs), and CO_2 adsorption. Since the main goal of this contribution is to discuss the merits of CTNCs with respect to other approaches in the synthesis of nitrogen-rich electroactive carbons, a particularly strong emphasis will be placed on the critical overview of the other strategies.

1.2 Electronic Properties of Graphene Edges

The electronic structure of nanographenes is predominantly controlled by quantum confinement effects [25] and edge effects [26–30], with the latter providing particular opportunities for chemical tunability. It has been shown computationally

that when graphene is spatially confined to the nanometer scale in two dimensions (nanographene), a density of states (DOS) arises at the Fermi level [27, 31–33]. These states (HOMO/LUMO) are non-bonding and are predominantly localized at the zigzag edges. Their existence has been subsequently confirmed using scanning tunneling spectroscopy [34, 35] and EPR [36, 37]. The nonbonding character of zigzag edge states leads to unconventional magnetic properties [38] and can be a source of enhanced (electro)chemical activity [5, 39]. In particular, the high electron density of the HOMO along the zigzag edges and their high polarizability make them susceptible to oxidation or other functionalizations [29, 40–42].

So far, electronic calculations for edge-substituted nanographenes have been primarily focused on the π-electron system. For nitrogen substitution, the primary conclusions were that the edge location is the most stable one [43] and that edge nitrogen p_z electrons would also have nonbonding character, with the Fermi level shifted accordingly to the higher electronegativity of nitrogen sites [43–45]. It is also recognized that electronic communication between a lone pair of pyridinic species and a π-electron system should lead to high (electro)chemical activity, desirable in many applications [46].

1.3 Edge Functionalization of Graphene

The strategies for inclusion of nitrogen functionalities at graphene edges can be divided into two groups: (i) a post-pyrolysis procedure via reaction of the carbon material with N-containing gases [44, 47–49] and (ii) carbonization of N-rich precursors [50–58]. Below we briefly discuss the extent to which these approaches address the challenges associated with the control over the location and nature of the N-functionalities in carbon material and with assuring their electrochemical availability.

1.3.1 Post-Pyrolysis Nitrogen Doping

The most common form of post-pyrolysis N-doping is through reaction of the carbon material with ammonia at high temperatures [44, 47, 59–61]. The advantage of this approach is its simplicity and avoidance of any oxygen-containing reactants. However, the corrosive nature of ammonia prevents its use in conventional templating methods using silica or zeolites. Chemical vapor deposition used to incorporate nitrogen into the graphitic lattice introduces primarily quaternary nitrogens [49, 62] while "softer" techniques have been shown to preferentially functionalize the edges and defect sites [44, 45, 63]. One of such "soft" (i.e., low temperature) and versatile approaches to post-pyrolysis edge chemistry involves the selective introduction of azides onto graphene edges through reaction with iodine azide [64] followed by click chemistry [65]. The diversity of alkynes that are commensurable with click chemistry makes this approach particularly promising for the future of tunable carbon materials.

1.3.2 Pyrolysis of Nitrogen-Containing Precursors

An alternative approach to N-rich graphitic material is through the pyrolysis of N-containing precursors. The most common precursor materials used to this end are melamine [54], vinylpyridine resin [66], urea [67], silk fibroin [68], and PAN [9–11, 13, 14, 53, 58, 69–77], some of which offer little N-functionality specificity. An

example of molecularly precise placement of nitrogen on the edges of nanographene involves the use of a bottom-up synthetic approach based on a cyclodehydrogenation of branched oligophenylenes [4], which allows for the exact control of shape (including armchair vs zigzag edges [78]), size [79], and functionality. Incorporation of nitrogen can be accomplished here in a straightforward manner by replacement of some of the phenylenes with nitrogen heterocycles, for example, pyrimidines [80]. Activity of such introduced edge nitrogens has been confirmed by demonstrating their ability to complex Pd(II) and Ru(II) metal salts [80].

Another example of molecularly precise nitrogen-rich carbon is graphitic carbon nitride (g-C_3N_4), usually consisting of tri-connected triazine units, which also represents the upper limit of nitrogen doping in sp^2 hybridized systems. Despite the fact that its polymeric derivative is one of the oldest reported synthetic polymers [81] and that there are many synthetic approaches [82–84], this well-defined semiconductor has only recently found use as a metal-free catalyst in electrochemical reactions [84–91]. One particularly intriguing aspect of g-C_3N_4 is that its molecular framework contains multiple sites that can be utilized for different catalytic functions [84] and can be manipulated to tune the electronic properties [92]. Moreover, it is highly amenable to further modification, for example, through the incorporation of other heteroatoms such as boron and phosphorus [93–96].

1.3.2.1 Polyacrylonitrile

The previous two examples illustrated how the structure of N-doped nanographene can be controlled by the molecular structure of the carbon precursor. Another example of a system that relies on (partial) retention of the elements of molecular architecture is PAN, one of the most commonly used precursors for the production of carbon fibers [58, 97, 98]. The key requirement for carbon precursors used for this purpose is their ability to exhibit a high degree of molecular orientation and to translate it upon carbonization into the orientation of partially graphitic domains. As shown in Scheme 1.1, with PAN this retention is achieved through the stabilization, which involves heat treatment in air between 200 and 300 °C resulting in cyclization of the nitrile groups and formation of

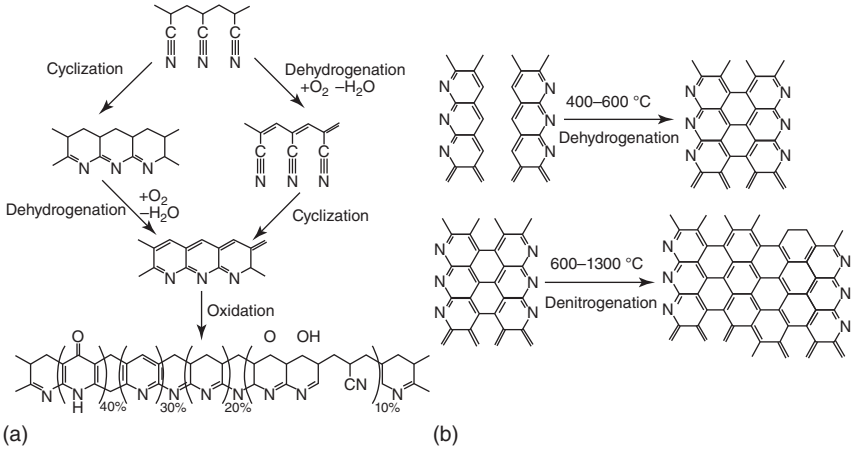

Scheme 1.1 Accepted mechanisms of PAN stabilization (a) and carbonization (b) [24].

a cross-linked ladder polymer primarily consisting of adjacent pyridines and pyridones [24]. Following this step, carbonization is carried out by pyrolysis under inert atmosphere, and proceeds by dehydrogenation (400–600 °C) followed by denitrogenation (>600 °C) [24].

The unique aspect of carbon from PAN is the location of the remaining nitrogens inferred primarily from X-ray photoelectron spectroscopy (XPS) studies of the evolution of nitrogen functionalities upon heat treatment. At lower carbonization temperatures (600–800 °C), pyridinic and pyridonic species (Scheme 1.1) represent the majority of the nitrogen functionalities (70–80%). Further heat treatment (>900 °C) introduces a small component of nitrogens into the basal plane of the nanographenes in a quaternary state. In recent years, high pyridinic nitrogen content in carbons obtained from PAN placed them in the center of the field of N-doped carbons [9, 10, 13, 16–18, 53, 58, 73, 99–102]. Assuring the (electro)chemical availability of nitrogen species remains, however, a major challenge with these materials.

1.4 Block Copolymer Templating as a Path to High Surface Area N-Doped Carbons with Accessible Nitrogen-Containing Graphitic Edges

As discussed above, control over the nanostructure and the molecular orientation is necessary to maximize the impact of the N-edge functionalities. The control of nanostructure is primarily required to assure high surface area of the material, which is the prerequisite of accessibility of N-edge functionalities. Ultimately, however, their wide electrochemical availability necessitates some level of control over the molecular orientation of nanographitic domains with respect to pore walls.

A common path to introducing porosity and to simultaneously control the pore size distribution is through a templating approach, where a well-defined scaffolding material is impregnated with the carbon precursor. The choice of template varies depending mainly on the size of the nanostructure desired. Porous carbon materials containing micropores (pores < 2 nm), mesopores (2–50 nm), and macropores (>50 nm) have been repeatedly demonstrated. The templates are mostly comprised of inorganics such as zeolites [103–107] or silica [11, 17, 20, 76, 108–111], and are removed after carbonization, for example, by acid wash. This approach, however, does not offer much control over the orientation of nanographenes within carbon domains.

An example of the process that allows control over the graphitic orientation is formation of carbon fibers from high carbon yield precursors such as PAN [99, 112] and mesophase-pitch [113]. In such systems graphitic planes typically adopt axial orientation, with possible additional degrees of order (e.g., radial arrangement for mesophase pitch-derived fibers [114]). Although such orientation may result in some exposure of nanographene edges on the surface of the fiber, with the typical fiber dimensions in the range of hundreds of nanometers to several microns, most of the edges remain buried within the bulk of the material. In the remainder of this section, we describe how this dilemma can be solved by simultaneous introduction of porosity and local PAN orientation through the use of block copolymer templating.

The majority of templated synthesis of nanoporous carbons is based on inorganic templates, and relatively limited efforts have been dedicated to soft (organic–organic)

templating [9, 10, 13, 14, 16, 115, 116]. Templating using block copolymers containing PAN and an immiscible sacrificial block (primarily poly(*n*-butyl acrylate) – PBA) has been pioneered in the past decade in our laboratories, with major stimulation coming from the advances in the field of controlled radical polymerization, especially atom transfer radical polymerization [117–128], which opened the way to new and versatile methods for the synthesis of polymers of various architectures (blocks, stars, brushes, etc.) [117–121, 129–133].

The turning point in the development of this route has been the finding that once PAN-*b*-PBA copolymers develop well-defined nanostructures driven by the immiscibility of the blocks, the PAN phase can be thermally stabilized, just as in the process used in the formation of carbon fibers [9]. The degree of stabilization achieved in this way has been shown to be sufficient to facilitate the preservation of the nanostructure upon pyrolysis under inert atmosphere, with PAN domains converting into carbonaceous semi-graphitic phase and the sacrificial block volatilizing, leading to the formation of nanoporous structure (Figure 1.2). The scheme shown in Figure 1.2 points to an additional important aspect of carbonization of PAN-*b*-PBA copolymers: given their partial crystallinity [134–136], PAN domains can form two types of interfaces with the sacrificial block: (i) the covalently bonded interface, perpendicular to the direction of polymer chains and (ii) the non-bonded interface, comprised of the side boundaries of PAN crystallites. Given that, in analogy with carbon fibers, partial graphitization of thermally stabilized PAN domains can be expected to proceed along the polymer chains, this kind of interfacial anisotropy should be retained in the carbonized material. The main consequence of such anisotropy would be the preferential exposure of nitrogen-rich zigzag edges on pore walls originating from the non-bonded interface. Understandably, within such picture, the ultimate fraction of nitrogen-rich edges exposed on pore walls would strongly depend on the polymer morphology, with the minimal exposure expected for lamellar structures, for which the interface with the sacrificial block would be of primarily covalently bonded nature.

While the presented view of molecular orientation effects in PAN-*b*-PBA copolymers and the resultant CNTCs is somewhat simplistic, it is supported by the structural

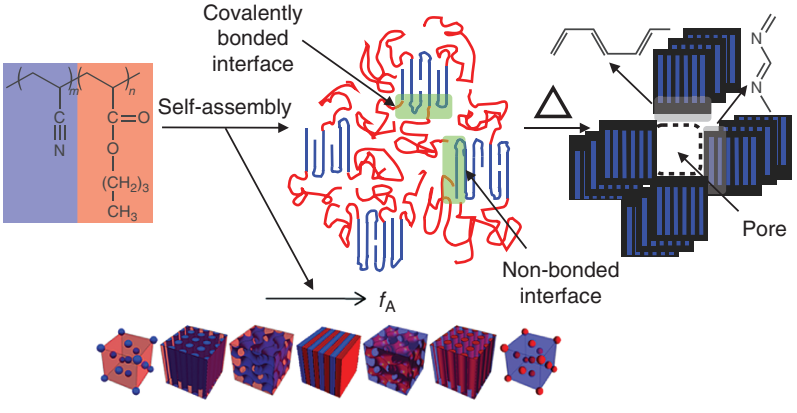

Figure 1.2 Nanometer-scale self-assembly and conversion of PAN-*b*-PBA to a nanoporous N-rich carbon material. The green shaded regions point to the two different types interfaces between the semicrystalline PAN and sacrificial block. ([8], Reproduced with permission of Wiley.)

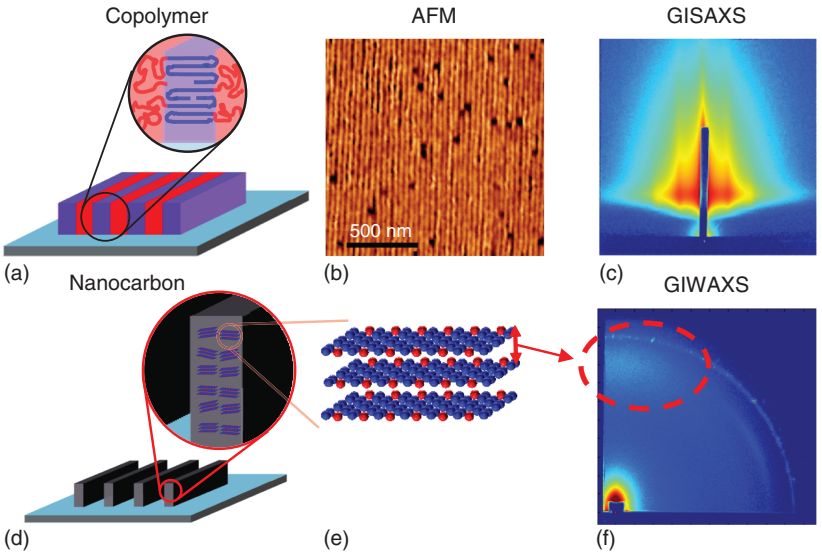

Figure 1.3 (a) Schematic, (b) AFM, and (c) grazing incidence small angle X-ray scattering (GISAXS) of a zone cast thin film of PBA-*b*-PAN and the (d) schematic, (e) comprising stacked nanographenes, and (f) grazing incidence wide angle X-ray scattering (GIWAXS) of the resultant lamellae CTNC film. ([8], Reproduced with permission of Wiley.)

analysis of highly ordered CNTCs obtained from ordered thin films of lamellar PAN-*b*-PBA copolymers prepared by zone casting [13, 137]. Atomic force microscopy (AFM) and grazing incidence small angle X-ray scattering (GISAXS) analysis of zone cast copolymer films (Figure 1.3a–c) and nanocarbons (not shown) revealed the presence of extended, parallel, narrow lamellae perpendicular to the substrate [13, 137]. As illustrated schematically in Figure 1.3a, for a copolymer this kind of structure implies the orientation of PAN chains parallel to the substrate. Analogous anisotropy and in-plane orientation of nanographitic domains in nanocarbon prepared from such ordered copolymer films was evident from the out-of plane position of the broad $\pi-\pi$ stacking (002) peak in grazing incidence wide angle X-ray scattering (GIWAXS) patterns of nanocarbon (Figure 1.3f).

The high degree of preservation of the lamellar nanostructure upon carbonization shown in the last example was facilitated by the presence of the supporting substrate. In the bulk, most morphologies, with the exception of some branching bicontinuous structures, after removal of the sacrificial block typically lead to various degrees of collapse of the three-dimensional nanostructure. The range of copolymer compositions assuring the preservation of nanoscale morphology in the bulk through the presence of contiguous PAN framework has been identified only recently. Small angle X-ray scattering (SAXS) patterns for the copolymer and nanocarbon show evidence of such preservation (Figure 1.4a). The high degree of nanostructure preservation upon carbonization of copolymers within this composition range has been confirmed through detailed analysis of SAXS patterns and nitrogen sorption isotherms.

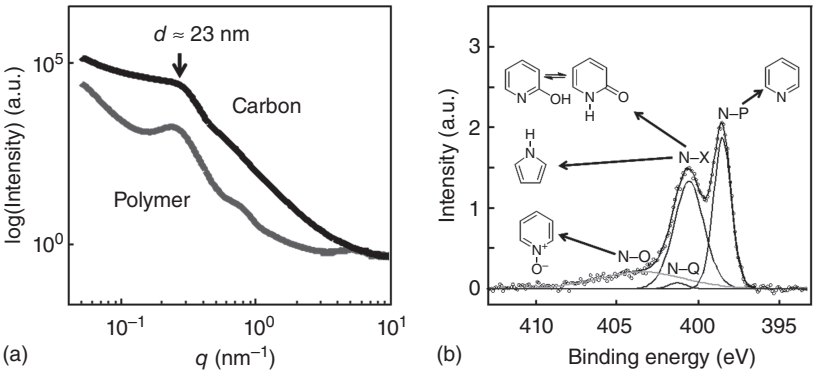

Figure 1.4 (a) Small angle X-ray scattering profiles of AN_{99}-*b*-BA_{70} annealed at 200 °C (dashed) and its corresponding CTNC pyrolyzed at 700 °C (solid). (b) XPS high resolution N 1s spectra of mesoporous carbon prepared from AN_{99}-*b*-BA_{70}. ([8], Reproduced with permission of Wiley.)

One of the particularly interesting structural insights into the environment of pyridinic nitrogens in such prepared materials came from the shape of their N 1s XPS spectral peak, in which the pyridinic peaks were particularly well resolved, with the full width at half maximum (FWHM) after deconvolution equal to about 1.2 eV (Figure 1.4b). This value is considerably lower than one reported for typical PAN-derived carbons such as electrospun carbon fibers (FWHM ~ 2 eV) [57] or even for such well-defined systems as g-C_3N_4 (FWHM ~ 1.5–2 eV) [138]. Since the width of the XPS peak reflects the heterogeneity of the chemical environment of any given species [139, 140], the uniquely narrow width observed for porous nanocarbons discussed here is a strong indication of "clean" exposure of N-containing edges on the pore walls. As described in the remaining sections of this article, high performance of such obtained materials as electrodes for supercapacitors and for oxygen reduction reaction, and as CO_2 sorbents, appears to confirm the high (electro)chemical availability of pyridinic nitrogens facilitated by such "clean" exposure.

1.5 Evidence of Enhanced Electrochemical Performance of Nitrogen-Rich Copolymer-Templated Mesoporous Carbons

1.5.1 Supercapacitors

Supercapacitors are an attractive energy storage device owing to their high power density at energy densities far above those of conventional capacitors [100]. Since supercapacitors store the electrical charge primarily in the electrical double layer (EDL) formed at the electrode/electrolyte interface [100], an ideal supercapacitor material should show a combination of high surface area (500–3000 $cm^2\ g^{-1}$) and high accessibility to the pore network.

The importance of high surface area as a factor determining the performance of supercapacitors is illustrated in Figure 1.5, which is a compilation of literature data on specific capacitance (in $F\ g^{-1}$) versus specific surface area (in $m^2\ g^{-1}$) for a wide range of porous

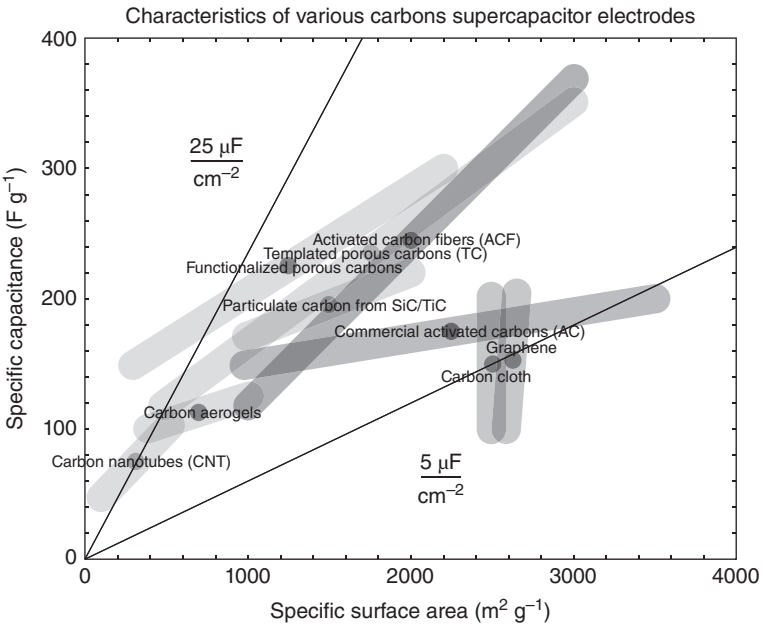

Figure 1.5 Summary plot of specific capacitance and specific surface area values for carbon materials commonly used in supercapacitors. ([8], Reproduced with permission of Wiley.)

carbon materials [141]. While the overall trend of the proportional increase of specific capacitance with the increase of specific surface area is quite clear, the results are broadly distributed, with most of the data points falling within the range of specific capacitances per unit area (C_{sa}) between 5 and 25 μF cm^{-2}, indicated in the plot by two solid lines. Typically, the EDL capacitance is viewed as being limited by the charge density attainable within the double layer, which, in turn depends on physicochemical characteristics of the electrolyte. For common electrolytes, the predicted range of EDL capacitance is between 15 and 25 μF cm^{-2}. Inspection of results summarized in Figure 1.5 shows that a considerable fraction of carbon materials exhibits EDL capacitances well below this range, which suggests that the DOS attainable in the *electrode* rather that within the *electrolyte* is the limiting factor.

There are strong indications that this limitation is related to the orientation of nanographitic domains with respect to pore walls. The primary argument supporting this view comes from the early experiments with electrodes fashioned from blocks of highly ordered pyrolitic graphite (HOPG), which showed a strong dependence of C_{sa} on basal plane orientation with respect to the electrode surface (3 μF cm^{-2} for face-on vs 50 μF cm^{-2} for edge-on orientation) [142]. More recent results with graphene-based supercapacitors, where the basal plane is expected to be a working surface, quote similarly low value of C_{sa} [1]. It should be emphasized that the dependence of C_{sa} on nanographene orientation fits well with the current understanding of the electronic structure of graphene, with edges (in particular zigzag) producing particularly high DOS [27, 31–33].

A widely used approach to increase the energy storage density in materials for supercapacitor electrodes relies on the introduction of an additional charge storage mechanism (pseudocapacitance), involving fast and reversible redox reactions. In carbon materials, this is usually accomplished through the incorporation of heteroatoms such as nitrogen or oxygen within the carbon framework [55, 57, 58, 69, 71, 143]. Pyridinic nitrogen functionalities are particularly sought after as a source of an effective Faradaic process, which involves protonation of the edge pyridinic functionality in acidic electrolyte, as shown in Figure 1.6.

In experiments with supercapacitors, the primary evidence of the benefits of enhanced accessibility of pyridinic nitrogens in CTNCs prepared from AN_{99}-*b*-BA_{70} with bicontinuous morphology comes from the observation that in acidic electrolytes they gave unusually high $C_{sa} = 33\ \mu F\ cm^{-2}$. The pseudocapacitive nature of this enhancement was evident in the characteristically distorted shape of cyclic voltammetry (CV) of carbons pyrolyzed at 700 °C (Figure 1.7a, dots). Consistently with the assignment of the origin of pseudocapacitance to pyridinic nitrogens, no C_{sa} enhancement or CV curve distortion was observed in a basic electrolyte (Figure 1.7a, circles). Further confirmation of the critical role of pyridinic nitrogens came from the CTNCs pyrolyzed at higher temperatures, which, as commonly reported in literature for PAN-derived carbons, exhibited loss of nitrogen content with the increase of pyrolysis temperature. As shown in Figure 1.7b, the C_{sa} for these materials decreased with the pyridinic nitrogen (N-P) content down to the "conventional" level of $\sim 15\ \mu F\ cm^{-2}$, with the shape of CV curve for the material

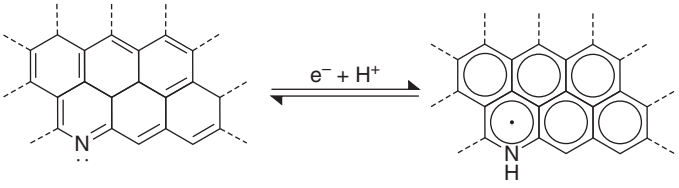

Figure 1.6 Possible pseudo-Faradaic reaction of the pyridinic group in acidic medium [144]. ([8], Reproduced with permission of Wiley.)

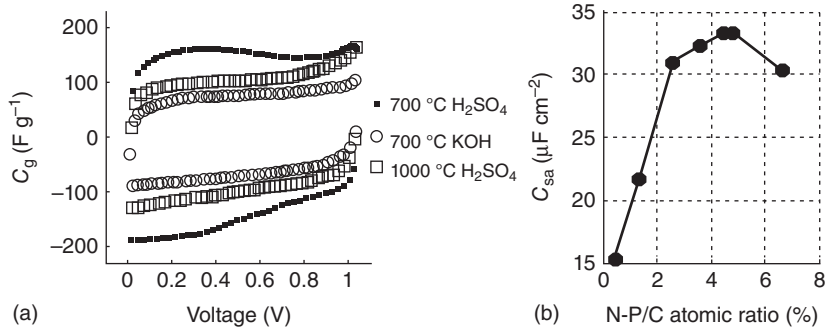

Figure 1.7 (a) Cyclic voltammetry of CTNCs from AN_{99}-*b*-BA_{70} at a scan rate of 2 mV s^{-1} using different pyrolysis temperatures (700 and 1000 °C) and electrolyte (H_2SO_4 and KOH). (b) Specific capacitance plots for CTNCs from AN_{99}-*b*-BA_{70} pyrolyzed at 700 °C in H_2SO_4 electrolyte as a function of pyridinic N-P/C atomic ratio %. ([8], Reproduced with permission of Wiley.)

pyrolyzed at 1000 °C no longer showing the clear distortion indicative of pseudocapacitance (Figure 1.7a, squares).

While similar overall dependence of C_{sa} on nitrogen content has been reported by other authors for N-doped carbons, unambiguous assignment of such trends to surface chemistry is usually impossible because of other factors, such as change of surface area and pore size distribution with pyrolysis conditions. This kind of ambiguity is not a major concern for the nanocarbons discussed here, since, based on SAXS, WAXS (wide angle X-ray scattering), and nitrogen adsorption studies, for pyrolysis temperatures ranging from 700 to 1000 °C, they exhibited remarkable insensitivity of nanostructure to pyrolysis conditions, which has been interpreted as the evidence of their robust bicontinuous morphology.

1.5.2 Metal-Free Oxygen Reduction Reaction

ORR is the crucial and rate-determining process in fuel cells [145] and considerable efforts are directed at the development of electrode systems facilitating its acceleration. Recent developments toward alternative cathodes, particularly non-metal systems, have led to the observed catalytic activity of a number of different N-rich carbons including carbon nitride [138], N-doped carbon nanotubes [46, 146, 147], graphene [148–150], and nanographenes [151, 152]. Although there are several explanations for the origin of the catalytic activity of N-rich nanocarbons, it is believed that the incorporation of nitrogen atoms into graphitic domain (especially pyridinic or/and graphitic nitrogen) plays a crucial role in the electrocatalytic performance [147, 150, 151, 153].

As shown in Figure 1.8, similar ORR activity has been observed when using CTNCs from AN_{99}-*b*-BA_{70} pyrolyzed at 700 °C, further confirming good electrochemical availability of nitrogen sites. The prominent reduction peak at −0.39 V is similar to those reported in other N-rich carbons [46]. Further work is currently underway to understand the influence of the nanoporous network on reduction rates and to determine whether the ORR occurs via a two- or four-electron process.

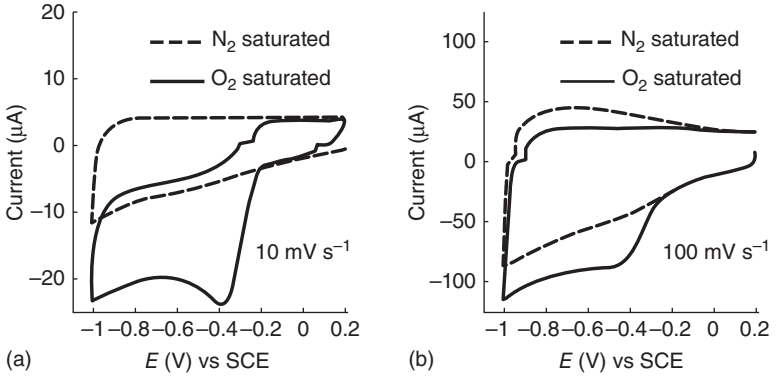

Figure 1.8 Cyclic voltammetry curves of oxygen reduction reaction experiments using nanoporous carbon from a AN_{99}-*b*-BA_{70} precursor at scan rates (a) 10 mV s^{-1} and (b) 100 mV s^{-1} in N_2 saturated and O_2 saturated 0.1 M KOH aqueous solution. ([8], Reproduced with permission of Wiley.)

1.6 CTNCs as CO_2 Sorbents

N-doped carbons are well suited for the selective capture of CO_2 gas. The basic nitrogens provide chemisorption sites [72, 154] that have been repeatedly shown to improve the adsorption capacity. Compared with the performance of traditional post-pyrolysis ammonia-treated porous carbon materials [155–157], N-doped carbons from N-rich precursors gain device stability by the incorporation of nitrogen into the carbon framework in the form of stable functionalities such as pyridinic, pyrolic, and quaternary nitrogen groups [158]. The precursors used so far for this application have been both small molecules [90] and polymers [102, 158, 159]. Controlled design of the porous structure can largely enhance the CO_2 capture performance. High surface area carbon nitride spheres [90] and N-doped carbon monoliths [158] were both found to exhibit competitive adsorptions capacities up to 2.9 and 4.4 mmol g^{-1} at room temperature, respectively.

As shown in Figure 1.9, despite its modest surface area (350 m^2 g^{-1}), CTNCs from AN_{99}-*b*-BA_{70} behaved as a relatively strong CO_2 sorbent, with adsorption capacity at 1 atm in the range of 2.0 mmol g^{-1}, comparable with other sorbents with much higher specific surface areas. Such high performance at modest specific area is reminiscent of enhanced performance of similar nanocarbon in supercapacitors (Section 1.5.1) and can be viewed as an evidence of enhanced chemisorption facilitated by unusually high accessibility of pyridinic nitrogens.

Strong support for this argument comes from the inspection of isosteric heat of adsorption curves (q_{st}), which provide the measure of the strength of the interaction between adsorbent and adsorbed species interaction at a given load (Figure 1.9b). Examination of literature data indicates that the typically reported values of q_{st} for physisorption of CO_2 in materials widely ranging from zeolites to porous carbons do not exceed 20–25 kJ mol^{-1} [160, 161]. Remarkably, at the initial uptake (0–0.2 mmol g^{-1}) the values of q_{st} for CTNCs were twice as high, only to gradually fall to the "conventional" level of ~25 kJ mol^{-1} with the increase of load (Figure 1.9b). Such behavior is highly

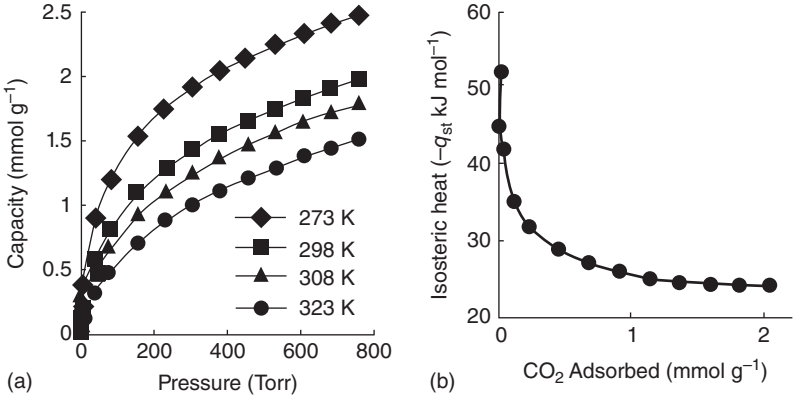

Figure 1.9 (a) CO_2 adsorption isotherms of nanoporous carbon prepared from AN_{99}-*b*-BA_{70} pyrolyzed at 700 °C. Solid lines through the data points are fits to the Langmuir–Freundlich equation [160]. (b) Calculated isosteric heat of CO_2 adsorption as a function of coverage. ([8], Reproduced with permission of Wiley.)

indicative of the presence of the limited surface fraction of strong chemisorption active sites (presumably pyridinic nitrogens), gradually saturating at higher loads.

1.7 Conclusions

Results presented in this chapter demonstrate how CTNC materials obtained by pyrolysis of block copolymers containing PAN (serving as a nitrogen-rich carbon source) and a sacrificial block can meet the challenges associated with creating porous carbon materials with control over the type of nitrogen functionalities and the accessibility of the active sites. The structural characteristics of CTNCs that allow them to meet this goal include (i) the high concentration of pyridinic functionalities resulting from the use of PAN as carbon source; (ii) stable nanostructure achievable with copolymer compositions affording robust bicontinuous morphology; and (iii) the "clean" exposure of nitrogen-containing zigzag edges of nanographitic domains on nanopore walls (inferred from the narrow pyridinic line-widths in the N 1s XPS spectra). We propose that the latter is facilitated in bicontinuous morphologies by the high occurrence of side-on orientation of PAN precursor crystallites with respect to the interfaces converted upon pyrolysis into nanopore walls. Such unusually "clean" exposure of pyridinic nitrogens appears to be the primary factor behind the fact that, despite their modest specific areas (below 500 $m^2 g^{-1}$), CTNCs exhibited levels of (electro)chemical performance comparable with carbons with specific surface areas at least twice as high. It is expected that further optimization of electrochemical performance of CTNCs (primarily through the choice of copolymer compositions leading to higher specific surface areas) will allow them to surpass the performance of other nitrogen-rich carbons. The simplicity and high level of control of the CTNC synthesis, as well as anticipated ease of its scale-up, further add to high promise of this class of materials.

Acknowledgments

Financial support was provided by the National Science Foundation (DMR-0304508 and DMR 09-69301), the Air Force Office of Scientific Research, and Carnegie Mellon University. A portion of this work was carried out at the Cornell High Energy Synchrotron Source (CHESS), Cornell University, which is partially supported by the National Science Foundation (DMR-0936384).

References

1 Stoller, M.D., Park, S., Zhu, Y., An, J., and Ruoff, R.S. (2008) *Nano Lett.*, **8**, 3498.
2 Li, X.L., Wang, X.R., Zhang, L., Lee, S.W., and Dai, H.J. (2008) *Science*, **319**, 1229.
3 Kosynkin, D.V., Higginbotham, A.L., Sinitskii, A., Lomeda, J.R., Dimiev, A., Price, B.K., and Tour, J.M. (2009) *Nature*, **458**, 872.
4 Wu, J.S., Pisula, W., and Mullen, K. (2007) *Chem. Rev.*, **107**, 718.
5 Beguin, F. and Frackowiak, E. (eds) (2010) *Carbons for Electrochemical Energy Storage and Conversion Systems*, Advanced Materials and Technologies, CRC Press, Boca Raton, FL.

6 Su, D.S. and Schlogl, R. (2010) *ChemSusChem*, **3**, 136.
7 Ruoff, R. (2008) *Nat. Nanotechnol.*, **3**, 10.
8 McGann, J.P., Zhong, M., Kim, E.K., Natesakhawat, S., Jaroniec, M., Whitacre, J.F., Matyjaszewski, K., Kowalewski, T. (2012) *Macromol. Chem. Phys.*, **213**, 1078.
9 Kowalewski, T., Tsarevsky, N.V., and Matyjaszewski, K. (2002) *J. Am. Chem. Soc.*, **124**, 10632.
10 Tang, C., Qi, K., Wooley, K.L., Matyjaszewski, K., and Kowalewski, T. (2004) *Angew. Chem. Int. Ed.*, **43**, 2783.
11 Kruk, M., Dufour, B., Celer, E.B., Kowalewski, T., Jaroniec, M., and Matyjaszewski, K. (2005) *J. Phys. Chem. B*, **109**, 9216.
12 Tang, C.B., Tracz, A., Kruk, M., Matyjaszewski, K., and Kowalewski, T. (2005) *Polym. Prepr.*, **46**, 424.
13 Tang, C.B., Tracz, A., Kruk, M., Zhang, R., Smilgies, D.M., Matyjaszewski, K., and Kowalewski, T. (2005) *J. Am. Chem. Soc.*, **127**, 6918.
14 Kruk, M., Dufour, B., Celer, E.B., Kowalewski, T., Jaroniec, M., and Matyjaszewski, K. (2006) *Chem. Mater.*, **18**, 1417.
15 Bowles, S.E., Wu, W., Kowalewski, T., Schalnat, M.C., Davis, R.J., Pemberton, J.E., Shim, I., Korth, B.D., and Pyun, J. (2007) *J. Am. Chem. Soc.*, **129**, 8694.
16 Huang, J.Y., Tang, C.B., Lee, H., Kowalewski, T., and Matyjaszewski, K. (2007) *Macromol. Chem. Phys.*, **208**, 2312.
17 Kruk, M., Kohlhaas, K.M., Dufour, B., Celer, E.B., Jaroniec, M., Matyjaszewski, K., Ruoff, R.S., and Kowalewski, T. (2007) *Microporous Mesoporous Mater.*, **102**, 178.
18 Tang, C., Dufour, B., Kowalewski, T., and Matyjaszewski, K. (2007) *Macromolecules*, **40**, 6199.
19 Aimi, J., McCullough, L.A., McGann, J.P., Kowalewski, T., and Matyjaszewski, K. (2008) *Polym. Prepr.*, **49**, 343.
20 Tang, C., Bombalskil, L., Kruk, M., Jaroniec, M., Matyjaszewski, K., and Kowalewski, T. (2008) *Adv. Mater.*, **20**, 1516.
21 Kulkarni, R., McCullough, L.A., Kowalewski, T., and Porter, L.M. (2009) *Synth. Met.*, **159**, 177.
22 Wu, D., Dong, H., Pietrasik, J., Kim, E.K., Hui, C.M., Zhong, M., Jaroniec, M., Kowalewski, T., and Matyjaszewski, K. (2011) *Chem. Mater.*, **23**, 2024.
23 Wu, D., Hui, C.M., Dong, H., Pietrasik, J., Ryu, H.J., Li, Z., Zhong, M., He, H., Kim, E.K., Jaroniec, M., Kowalewski, T., and Matyjaszewski, K. (2011) *Macromolecules*, **44**, 5846.
24 Bajaj, P. and Roopanwal, A.K. (1997) *J. Macromol. Sci., Rev. Macromol. Chem. Phys.*, **C37**, 97.
25 Gao, X.F., Zhou, Z., Zhao, Y.L., Nagase, S., Zhang, S.B., and Chen, Z.F. (2008) *J. Phys. Chem. C*, **112**, 12677.
26 Basu, D., Gilbert, M.J., Register, L.F., Banerjee, S.K., and MacDonald, A.H. (2008) *Appl. Phys. Lett.*, **92**, 042114.
27 Fujita, M., Wakabayashi, K., Nakada, K., and Kusakabe, K. (1996) *J. Phys. Soc. Jpn.*, **65**, 1920.
28 Pollet, R. and Amara, H. (2009) *J. Chem. Theory Comput.*, **5**, 1719.
29 Radovic, L.R. and Bockrath, B. (2005) *J. Am. Chem. Soc.*, **127**, 5917.
30 Wakabayashi, K., Takane, Y., Yamamoto, M., and Sigrist, M. (2009) *Carbon*, **47**, 124.
31 Klein, D.J. (1994) *Chem. Phys. Lett.*, **217**, 261.

32 Kobayashi, K. (1993) *Phys. Rev. B*, **48**, 1757.
33 Nakada, K., Fujita, M., Dresselhaus, G., and Dresselhaus, M.S. (1996) *Phys. Rev. B*, **54**, 17954.
34 Kobayashi, Y., Fukui, K.-I., Enoki, T., Kusakabe, K., and Kaburagi, Y. (2005) *Phys. Rev. B*, **71**, 193406.
35 Niimi, Y., Matsui, T., Kambara, H., Tagami, K., Tsukada, M., and Fukuyama, H. (2006) *Phys. Rev. B*, **73**, 085421.
36 Joly, V.L.J., Kiguchi, M., Hao, S.-J., Takai, K., Enoki, T., Sumii, R., Amemiya, K., Muramatsu, H., Hayashi, T., Kim, Y.A., Endo, M., Campos-Delgado, J., Lopez-Urias, F., Botello-Mendez, A., Terrones, H., Terrones, M., and Dresselhaus, M.S. (2010) *Phys. Rev. B*, **81**, 245428.
37 Joly, V.L.J., Takahara, K., Takai, K., Sugihara, K., Enoki, T., Koshino, M., and Tanaka, H. (2010) *Phys. Rev. B*, **81**, 115408.
38 Kan, E.J., Li, Z.Y., Yang, J.L., and Hou, J.G. (2008) *J. Am. Chem. Soc.*, **130**, 4224.
39 Jaing, D., Gao, X., Nagase, S., and Chen, Z. (2010) in *Chemistry of Nanocarbons* (eds T. Akasaka, F. Wudl, and S. Nagase), John Wiley & Sons, Ltd, West Sussex.
40 Jiang, D.E., Sumpter, B.G., and Dai, S. (2006) *J. Phys. Chem. B*, **110**, 23628.
41 Jiang, D.-E., Sumpter, B.G., and Dai, S. (2007) *J. Chem. Phys.*, **126**, 134701.
42 Stein, S.E. and Brown, R.L. (1987) *J. Am. Chem. Soc.*, **109**, 3721.
43 Yu, S.S., Zheng, W.T., Wen, Q.B., and Jiang, Q. (2008) *Carbon*, **46**, 537.
44 Wang, X., Li, X., Zhang, L., Yoon, Y., Weber, P.K., Wang, H., Guo, J., and Dai, H. (2009) *Science*, **324**, 768.
45 Li, X., Wang, H., Robinson, J.T., Sanchez, H., Diankov, G., and Dai, H. (2009) *J. Am. Chem. Soc.*, **131**, 15939.
46 Tang, Y., Allen, B.L., Kauffman, D.R., and Star, A. (2009) *J. Am. Chem. Soc.*, **131**, 13200.
47 Jansen, R.J.J. and Vanbekkum, H. (1994) *Carbon*, **32**, 1507.
48 Stohr, B., Boehm, H.P., and Schlogl, R. (1991) *Carbon*, **29**, 707.
49 Wei, D., Liu, Y., Wang, Y., Zhang, H., Huang, L., and Yu, G. (2009) *Nano Lett.*, **9**, 1752.
50 Raymundo-Pinero, E., Cazorla-Amoros, D., Linares-Solano, A., Find, J., Wild, U., and Schlogl, R. (2002) *Carbon*, **40**, 597.
51 Bimer, J., Satbut, P.D., Bertozecki, S., Boudou, J.P., Broniek, E., and Siemieniewska, T. (1998) *Fuel*, **77**, 519.
52 Draper, S.M., Gregg, D.J., and Madathil, R. (2002) *J. Am. Chem. Soc.*, **124**, 3486.
53 Hou, P.X., Orikasa, H., Yamazaki, T., Matsuoka, K., Tomita, A., Setoyama, N., Fukushima, Y., and Kyotani, T. (2005) *Chem. Mater.*, **17**, 5187.
54 Hulicova, D., Yamashita, J., Soneda, Y., Hatori, H., and Kodama, M. (2005) *Chem. Mater.*, **17**, 1241.
55 Hulicova-Jurcakova, D., Kodama, M., Shiraishi, S., Hatori, H., Zhu, Z.H., and Lu, G.Q. (2009) *Adv. Funct. Mater.*, **19**, 1800.
56 Lahaye, J., Nanse, G., Bagreev, A., and Strelko, V. (1999) *Carbon*, **37**, 585.
57 Lota, G., Grzyb, B., Machnikowska, H., Machnikowski, J., and Frackowiak, E. (2005) *Chem. Phys. Lett.*, **404**, 53.
58 Ra, E.J., Raymundo-Pinero, E., Lee, Y.H., and Beguin, F. (2009) *Carbon*, **47**, 2984.
59 Biniak, S., Szymanski, G., Siedlewski, J., and Swiatkowski, A. (1997) *Carbon*, **35**, 1799.

60 Boehm, H.P., Mair, G., Stoehr, T., Derincon, A.R., and Tereczki, B. (1984) *Fuel*, **63**, 1061.
61 Grant, K.A., Zhu, Q., and Thomas, K.M. (1994) *Carbon*, **32**, 883.
62 Wang, X., Liu, Y., Zhu, D., Zhang, L., Ma, H., Yao, N., and Zhang, B. (2002) *J. Phys. Chem. B*, **106**, 2186.
63 Quintana, M., Montellano, A., Castillo, A.E.D., Van Tendeloo, G., Bittencourt, C., and Prato, M. (2011) *Chem. Commun.*, **47**, 9330.
64 Devadoss, A. and Chidsey, C.E.D. (2007) *J. Am. Chem. Soc.*, **129**, 5370.
65 Sha, C.-K. and Mohanakrishnan, A.K. (2003) *Synthetic Applications of 1,3-Dipolar Cycloaddition Chemistry Toward Heterocycles and Natural Products* (eds Albert Padwa, William H. Pearson), John Wiley & Sons, Inc., p. 623.
66 Grzyb, B., Machnikowski, J., and Weber, J.V. (2004) *J. Anal. Appl. Pyrolysis*, **72**, 121.
67 Seredych, M., Hulicova-Jurcakova, D., Lu, G.Q., and Bandosz, T.J. (2008) *Carbon*, **46**, 1475.
68 Kim, Y.J., Abe, Y., Yanaglura, T., Park, K.C., Shimizu, M., Iwazaki, T., Nakagawa, S., Endo, M., and Dresselhaus, M.S. (2007) *Carbon*, **45**, 2116.
69 Frackowiak, E., Lota, G., Machnikowski, J., Vix-Guterl, C., and Beguin, F. (2006) *Electrochim. Acta*, **51**, 2209.
70 Gouerec, P., Talbi, H., Miousse, D., Tran-Van, F., Dao, L.H., and Lee, K.H. (2001) *J. Electrochem. Soc.*, **148**, A94.
71 Kim, C., Ngoc, B.T.N., Yang, K.S., Kojima, M., Kim, Y.A., Kim, Y.J., Endo, M., and Yang, S.C. (2007) *Adv. Mater.*, **19**, 2341.
72 Pels, J.R., Kapteijn, F., Moulijn, J.A., Zhu, Q., and Thomas, K.M. (1995) *Carbon*, **33**, 1641.
73 Xu, B., Wu, F., Chen, S., Zhang, C.Z., Cao, G.P., and Yang, Y.S. (2007) *Electrochim. Acta*, **52**, 4595.
74 Machnikowski, J., Grzyb, B., Weber, J.V., Frackowiak, E., Rouzaud, J.N., and Beguin, F. (2004) *Electrochim. Acta*, **49**, 423.
75 Zhou, C.F., Liu, T., Wang, T., and Kumar, S. (2006) *Polymer*, **47**, 5831.
76 Kruk, M., Dufour, B., Celer, E.B., Kowalewski, T., Jaroniec, M., and Matyjaszewski, K. (2008) *Macromolecules*, **41**, 8584.
77 Pyun, J., Jia, S.J., Kowalewski, T., Patterson, G.D., and Matyjaszewski, K. (2003) *Macromolecules*, **36**, 5094.
78 Kastler, M., Schmidt, J., Pisula, W., Sebastiani, D., and Müllen, K. (2006) *J. Am. Chem. Soc.*, **128**, 9526.
79 Fogel, Y., Zhi, L.J., Rouhanipour, A., Andrienko, D., Rader, H.J., and Mullen, K. (2009) *Macromolecules*, **42**, 6878.
80 Draper, S.M., Gregg, D.J., Schofield, E.R., Browne, W.R., Duati, M., Vos, J.G., and Passaniti, P. (2004) *J. Am. Chem. Soc.*, **126**, 8694.
81 Liebig, J. (1834) *Ann. Pharm.*, **10**, 10.
82 Horvath-Bordon, E., Kroke, E., Svoboda, I., Fuess, H., and Riedel, R. (2005) *New J. Chem.*, **29**, 693.
83 Kroke, E. and Schwarz, M. (2004) *Coord. Chem. Rev.*, **248**, 493.
84 Thomas, A., Fischer, A., Goettmann, F., Antonietti, M., Muller, J.-O., Schlogl, R., and Carlsson, J.M. (2008) *J. Mater. Chem.*, **18**, 4893.
85 Li, Y., Zhang, J., Wang, Q., Jin, Y., Huang, D., Cui, Q., and Zou, G. (2010) *J. Phys. Chem. B*, **114**, 9429.

86 Liu, G., Niu, P., Sun, C., Smith, S.C., Chen, Z., Lu, G.Q., and Cheng, H.-M. (2010) *J. Am. Chem. Soc.*, **132**, 11642.
87 Zhu, J., Wei, Y., Chen, W., Zhao, Z., and Thomas, A. (2010) *Chem. Commun.*, **46**, 6965.
88 Goettmann, F., Fischer, A., Antonietti, M., and Thomas, A. (2006) *Chem. Commun.*, 4530.
89 Goettmann, F., Thomas, A., and Antonietti, M. (2007) *Angew. Chem. Int. Ed.*, **46**, 2717.
90 Li, Q., Yang, J., Feng, D., Wu, Z., Wu, Q., Park, S., Ha, C.-S., and Zhao, D. (2010) *Nano Res.*, **3**, 632.
91 Vayner, E. and Anderson, A.B. (2007) *J. Phys. Chem. C*, **111**, 9330.
92 Li, X.-H., Zhang, J., Chen, X., Fischer, A., Thomas, A., Antonietti, M., and Wang, X. (2011) *Chem. Mater.*, **23**, 4344.
93 Zhang, Y., Mori, T., Ye, J., and Antonietti, M. (2010) *J. Am. Chem. Soc.*, **132**, 6294.
94 Wang, Y., Zhang, J., Wang, X., Antonietti, M., and Li, H. (2010) *Angew. Chem. Int. Ed.*, **49**, 3356.
95 Wang, Y., Li, H., Yao, J., Wang, X., and Antonietti, M. (2011) *Chem. Sci.*, **2**, 446.
96 Zhang, J., Sun, J., Maeda, K., Domen, K., Liu, P., Antonietti, M., Fu, X., and Wang, X. (2011) *Energy Environ. Sci.*, **4**, 675.
97 Donnet, J., Wang, T.K., Peng, J.C.M., and Rebouillat, S. (1998) *Carbon Fibers*, Marcel Dekker, New York.
98 Ryu, Z.Y., Rong, H.Q., Zheng, J.T., Wang, M.Z., and Zhang, B.J. (2002) *Carbon*, **40**, 1144.
99 Fernandez-Saavedra, R., Aranda, P., and Ruiz-Hitzky, E. (2004) *Adv. Funct. Mater.*, **14**, 77.
100 Conway, B.E. (1999) *Electrochemical Supercapacitors: Scientific Fundamentals and Technological Applications*, Kluwer Academic/Plenum Publishers, New York.
101 Yang, X., Wu, D., Chen, X., and Fu, R. (2010) *J. Phys. Chem. C*, **114**, 8581.
102 Shen, W., Zhang, S., He, Y., Li, J., and Fan, W. (2011) *J. Mater. Chem.*, **21**, 14036.
103 Ania, C.O., Khomenko, V., Raymundo-Piñero, E., Parra, J.B., and Béguin, F. (2007) *Adv. Funct. Mater.*, **17**, 1828.
104 Johnson, S.A., Brigham, E.S., Ollivier, P.J., and Mallouk, T.E. (1997) *Chem. Mater.*, **9**, 2448.
105 Kyotani, T., Nagai, T., Inoue, S., and Tomita, A. (1997) *Chem. Mater.*, **9**, 609.
106 Ma, Z.X., Kyotani, T., and Tomita, A. (2000) *Chem. Commun.*, 2365.
107 Sakintuna, B., Aktas, Z., and Yurum, Y. (2003) *Abstr. Pap. Am. Chem. Soc.*, **226**, U538.
108 Kawashima, D., Aihara, T., Kobayashi, Y., Kyotani, T., and Tomita, A. (2000) *Chem. Mater.*, **12**, 3397.
109 Kim, J.Y., Yoon, S.B., and Yu, J.S. (2003) *Chem. Mater.*, **15**, 1932.
110 Paraknowitsch, J.P., Zhang, Y., and Thomas, A. (2011) *J. Mater. Chem.*, **21**, 15537.
111 Fuertes, A.B., Lota, G., Centeno, T.A., and Frackowiak, E. (2005) *Electrochim. Acta*, **50**, 2799.
112 Jang, J. and Bae, J. (2004) *Angew. Chem. Int. Ed.*, **43**, 3803.
113 Inagaki, M. and Kang, F. (2006) *Carbon Materials Science and Engineering*, Tsinghua University Press, Beijing, p. 359.

114 Inagaki, M. (2010) in *Carbons for Electrochemical Energy Storage and Conversion Systems* (eds F. Beguin and E. Frackowiak), CRC Press, Boca Raton, FL, p. 37.
115 Liang, C.D., Hong, K.L., Guiochon, G.A., Mays, J.W., and Dai, S. (2004) *Angew. Chem. Int. Ed.*, **43**, 5785.
116 Xu, F., Cai, R., Zeng, Q., Zou, C., Wu, D., Li, F., Lu, X., Liang, Y., and Fu, R. (2011) *J. Mater. Chem.*, **21**, 1970.
117 di Lena, F. and Matyjaszewski, K. (2010) *Prog. Polym. Sci.*, **35**, 959.
118 Gao, H. and Matyjaszewski, K. (2009) *Prog. Polym. Sci.*, **34**, 317.
119 Lee, H.-I., Pietrasik, J., Sheiko, S.S., and Matyjaszewski, K. (2010) *Prog. Polym. Sci.*, **35**, 24.
120 Matyjaszewski, K. (2005) *Prog. Polym. Sci.*, **30**, 858.
121 Sheiko, S.S., Sumerlin, B.S., and Matyjaszewski, K. (2008) *Prog. Polym. Sci.*, **33**, 759.
122 Dufour, B., Tang, C., Koynov, K., Zhang, Y., Pakula, T., and Matyjaszewski, K. (2008) *Macromolecules*, **41**, 2451.
123 Kowalewski, T., Tang, C., Kruk, M., Dufour, B., and Matyjaszewski, K. (2006) *ACS Symp. Ser.*, **944**, 295.
124 Kruk, M., Tang, C., Dufour, B., Matyjaszewski, K., and Kowalewski, T. (eds) (2006) *Block Copolymers in Nanoscience*, Wiley-VCH Verlag GmbH, Weinheim.
125 Matyjaszewski, K., Jo, S.M., Paik, H.-J., and Gaynor, S.G. (1997) *Macromolecules*, **30**, 6398.
126 Matyjaszewski, K., Jo, S.M., Paik, H.-J., and Shipp, D.A. (1999) *Macromolecules*, **32**, 6431.
127 Tang, C., Kowalewski, T., and Matyjaszewski, K. (2003) *Macromolecules*, **36**, 8587.
128 Tang, C., Kowalewski, T., and Matyjaszewski, K. (2003) *Macromolecules*, **36**, 1465.
129 Braunecker, W.A. and Matyjaszewski, K. (2007) *Prog. Polym. Sci.*, **32**, 93.
130 Matyjaszewski, K. and Tsarevsky, N.V. (2009) *Nat. Chem.*, **1**, 276.
131 Matyjaszewski, K. and Xia, J. (2001) *Chem. Rev.*, **101**, 2921.
132 Siegwart, D.J., Oh, J.K., and Matyjaszewski, K. (2012) *Prog. Polym. Sci.*, **37**, 18.
133 Tsarevsky, N.V. and Matyjaszewski, K. (2007) *Chem. Rev.*, **107**, 2270.
134 Hobson, R.J. and Windle, A.H. (1993) *Macromolecules*, **26**, 6903.
135 Liu, X.D. and Ruland, W. (1993) *Macromolecules*, **26**, 3030.
136 Sawai, D., Yamane, A., Kameda, T., Kanamoto, T., Ito, M., Yamazaki, H., and Hisatani, K. (1999) *Macromolecules*, **32**, 5622.
137 Tang, C., Wu, W., Smilgies, D.-M., Matyjaszewski, K., and Kowalewski, T. (2011) *J. Am. Chem. Soc.*, **133**, 11802.
138 Yang, S., Feng, X., Wang, X., and Müllen, K. (2011) *Angew. Chem. Int. Ed.*, **50**, 5339.
139 Briggs, D. and Beamson, G. (1993) *Anal. Chem.*, **65**, 1517.
140 Hughes, H.P. and Starnberg, H.I. (2001) *Electron Spectroscopies Applied to Low-Dimensional Materials*, Kluwer Academic Publishers, Norwell, MA.
141 Zhang, L.L., Zhou, R., and Zhao, X.S. (2010) *J. Mater. Chem.*, **20**, 5983.
142 Randin, J.P. and Yeager, E. (1972) *J. Electroanal. Chem.*, **36**, 257.
143 Beguin, F., Szostak, K., Lota, G., and Frackowiak, E. (2005) *Adv. Mater.*, **17**, 2380.
144 Frackowiak, E. (2007) *Phys. Chem. Chem. Phys.*, **9**, 1774.
145 Su, D.S. and Sun, G. (2011) *Angew. Chem. Int. Ed.*, **50**, 11570.
146 Gong, K., Du, F., Xia, Z., Durstock, M., and Dai, L. (2009) *Science*, **323**, 760.
147 Yu, D., Zhang, Q., and Dai, L. (2010) *J. Am. Chem. Soc.*, **132**, 15127.

148 Qu, L., Liu, Y., Baek, J.-B., and Dai, L. (2010) *ACS Nano*, **4**, 1321.
149 Wang, Y., Shao, Y., Matson, D.W., Li, J., and Lin, Y. (2010) *ACS Nano*, **4**, 1790.
150 Sidik, R.A., Anderson, A.B., Subramanian, N.P., Kumaraguru, S.P., and Popov, B.N. (2006) *J. Phys. Chem. B*, **110**, 1787.
151 Liu, R., Wu, D., Feng, X., and Müllen, K. (2010) *Angew. Chem. Int. Ed.*, **49**, 2565.
152 Li, Y., Zhao, Y., Cheng, H., Hu, Y., Shi, G., Dai, L., and Qu, L. (2011) *J. Am. Chem. Soc.*, **134**, 15.
153 Ikeda, T., Boero, M., Huang, S.-F., Terakura, K., Oshima, M., and Ozaki, J.-I. (2008) *J. Phys. Chem. C*, **112**, 14706.
154 Hiyoshi, N., Yogo, K., and Yashima, T. (2005) *Microporous Mesoporous Mater.*, **84**, 357.
155 D'Alessandro, D.M., Smit, B., and Long, J.R. (2010) *Angew. Chem. Int. Ed.*, **49**, 6058.
156 Pevida, C., Plaza, M.G., Arias, B., Fermoso, J., Rubiera, F., and Pis, J.J. (2008) *Appl. Surf. Sci.*, **254**, 7165.
157 Wang, Q., Luo, J., Zhong, Z., and Borgna, A. (2011) *Energy Environ. Sci.*, **4**, 42.
158 Hao, G.-P., Li, W.-C., Qian, D., and Lu, A.-H. (2010) *Adv. Mater.*, **22**, 853.
159 Sevilla, M., Valle-Vigon, P., and Fuertes, A.B. (2011) *Adv. Funct. Mater.*, **21**, 2781.
160 Natesakhawat, S., Culp, J.T., Matranga, C., and Bockrath, B. (2007) *J. Phys. Chem. C*, **111**, 1055.
161 Khelifa, A., Benchehida, L., and Derriche, Z. (2004) *J. Colloid Interface Sci.*, **278**, 9.